Kinetics and Mechanism of the Reaction of OH with ClO

YURI BEDJANIAN, VÉRONIQUE RIFFAULT, GEORGES LE BRAS

Laboratoire de Combustion et Systèmes Réactifs, CNRS *and Université d'Orléans*, 45071 *Orléans Cedex* 2, *France*

Received 7 February 2001; accepted 31 May 2001

ABSTRACT: The kinetics and mechanism of the following reactions have been studied in the temperature range 230–360 K and at total pressure of 1 Torr of helium, using the discharge-flow mass spectrometric method:

$$OH + ClO \longrightarrow Cl + HO_2 \quad (1a)$$

$$OH + ClO \longrightarrow HCl + O_2 \quad (1b)$$

The following Arrhenius expression for the total rate constant was obtained from the kinetics of OH consumption in excess of ClO radical, produced in the $Cl + O_3$ reaction either in excess of Cl atoms or ozone: $k_1 = (6.7 \pm 1.8) \times 10^{-12} \exp\{(360 \pm 90)/T\}$ cm^3 molecule^{-1} s^{-1} (with $k_1 = (2.2 \pm 0.4) \times 10^{-11}$ cm^3 molecule^{-1} s^{-1} at T = 298 K), where uncertainties represent 95% confidence limits and include estimated systematic errors. The value of k_1 is compared with those from previous studies and current recommendations. HCl was detected as a minor product of reaction (1) and the rate constant for the channel forming HCl (reaction (1b)) has been determined from the kinetics of HCl formation at T = 230–320 K: $k_{1b} = (9.7 \pm 4.1) \times 10^{-14} \exp\{(600 \pm 120)/T\}$ cm^3 molecule^{-1} s^{-1} (with $k_{1b} = (7.3 \pm 2.2) \times 10^{-13}$ cm^3 molecule^{-1} s^{-1} and $k_{1b}/k_1 = 0.035 \pm 0.010$ at T = 298 K), where uncertainties represent 95% confidence limits. In addition, the measured kinetic data were used to derive the enthalpy of formation of HO_2 radicals: $\Delta H_{f,298}(HO_2) = 3.0 \pm 0.4$ kcal mol^{-1}. © 2001 John Wiley & Sons, Inc. Int J Chem Kinet 33: 587–599, 2001

INTRODUCTION

Chlorine is recognized to be an efficient ozone destroyer in the stratosphere. Its efficiency strongly depends on the chlorine partitioning between its active forms (Cl, ClO) and inactive reservoir species (e.g. HCl). Although the stratospheric chlorine chemistry is fairly well known, there are still some unresolved questions. One of them is that the models fail to reproduce (they underestimate) the measured HCl-concentration profiles in the upper stratosphere. One possible explanation of the discrepancy is that an HCl source is missing in the models. In this respect the minor channel of reaction (1) between OH and ClO radicals was proposed as an additional source of HCl in the stratosphere [1]:

$$OH + ClO \longrightarrow Cl + HO_2 \qquad \Delta H = -(1.8 \pm 0.4)\,\text{kcal mol}^{-1} \quad (1a)$$

$$OH + ClO \longrightarrow HCl + O_2 \qquad \Delta H = -(55.8 \pm 0.4)\,\text{kcal mol}^{-1} \quad (1b)$$

Correspondence to: Yuri Bedjanian; e-mail: bedjanian@cnrs-orleans.fr.

(Enthalpy data are from Ref. [2], except $\Delta H_{f,298}$ $(HO_2) = 3.0 \pm 0.4$ kcal mol^{-1} determined in this work.) It was shown that a branching ratio of 7% for the HCl-forming channel (1b) would reconcile model calculations and HCl measurements [3–5].

In earlier studies of reaction (1), channel (1a) forming HO_2 and Cl has been shown to be the major pathway of the reaction [6–9]. In these studies the branching ratio k_{1a}/k_1 was reported to be in the range 0.65–1.0. However, the branching ratio for the HCl-forming channel was not measured and this channel was not ruled out. Only in the most recent study of Lipson et al. [10], where the kinetics of HCl formation in the reaction between OH and ClO was directly observed, the branching ratio for the channel (1b) was determined to be 0.07 ± 0.03, independent of temperature ($T = 207$–298 K) and pressure ($P = 94$–203 Torr). This experimental result is in contradiction with that from a recent theoretical study of the reaction (1) [11], where channel (1b) was found to be less important and experimentally observed HCl was suggested to be formed by the secondary reaction $HO_2 + Cl \rightarrow HCl + O_2$. Hence, the results of the unique experimental measurement of k_{1b}/k_1 needed to be confirmed.

The total rate constant of reaction (1) was measured in a number of studies [6–9,12–14]. The three earliest measurements [6,7,12] gave $k_1 \approx 10^{-11}$ cm^3 molecule^{-1} s^{-1} at room temperature. The rate constant was found to be independent of temperature at $T = 248$–335 K and 243–298 K in the Ref. [12] and [7], respectively. Significantly higher values of k_1(1.75×10^{-11} and 1.94×10^{-11} cm^3 molecule^{-1} s^{-1}) at $T = 298$ K have been measured by Hills and Howard [8] and by Poulet et al. [9], respectively. In addition, Hills and Howard [8] observed a negative temperature dependence of the rate constant with $E/R = -235$ K. A very similar value of the temperature factor ($E/R = -290$ K) but a somewhat lower value of k_1 (1.46×10^{-11} cm^3 molecule^{-1} s^{-1} at $T = 298$ K) were further measured by Lipson et al. [13]. Finally, in the most recent study by Kegley-Owen et al. [14] a much higher value of k_1 (2.4×10^{-11} cm^3 molecule^{-1} s^{-1} at room temperature) has been measured, although the temperature factor $E/R = -295$ K was found to be similar to that determined in Ref. [13]. Thus, although the temperature dependence of k_1 seems to be well established [8,13,14], a significant difference between the absolute values of k_1 exists (factor 1.6 for the two most recent studies [13,14]) and k_1 needs to be redetermined.

The present work reports the results of the experimental study of reaction (1) at $T = 230$–360 K, including the measurements of the total rate constant as well as of the rate constant for the HCl-forming channel of the reaction.

EXPERIMENTAL SECTION

Experiments were carried out in a discharge flow reactor, using a modulated molecular beam mass spectrometer as the detection method. The main reactor, shown in Fig. 1 along with the triple movable injector for the reactants, consisted of a Pyrex tube (45-cm length and 2.4-cm i.d.) with a jacket for the thermostated liquid circulation (water or ethanol). The walls of the reactor as well as of the injector were coated with halocarbon wax in order to minimize the heterogeneous loss of active species. All experiments were conducted at 1-Torr total pressure, helium being used as the carrier gas.

The fast reaction of H atoms with NO_2 was used as the source of OH radicals:

$$H + NO_2 \longrightarrow OH + NO \qquad (2)$$

($k_2 = 4.0 \times 10^{-10} \exp(-340/T)$ cm^3 molecule^{-1} s^{-1} [2]).

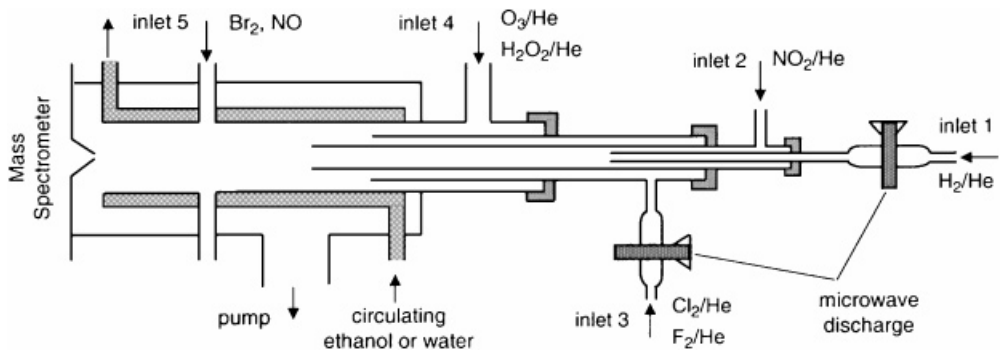

Figure 1 Diagram of the apparatus used.

NO_2 was always used in excess over H atoms, which were produced in a microwave discharge of H_2/He mixtures. In the study of the kinetics of reaction (1) where relatively low concentrations of OH were used (see below), OH radicals were detected as $HOBr^+$ ($m/e = 96/98$) after scavenging by an excess of Br_2 (added at the end of the reactor through inlet 5, located 5-cm upstream of the sampling cone) via reaction (3):

$$OH + Br_2 \longrightarrow Br + HOBr \qquad (3)$$

($k_3 = 1.8 \times 10^{-11} \exp(235/T)$ cm^3 molecule^{-1} s^{-1} [15]).

This method for OH detection was preferred to the direct detection of these radicals at $m/e = 17$ (OH^+) owing to a significant contribution of traces of water vapor at this peak. The same procedure of OH chemical conversion to HOBr was used for the measurements of the absolute concentrations: [OH] = [HOBr] = $\Delta[Br_2]$. Thus, OH concentrations were determined from the consumed fraction of Br_2 concentration. The concentration of Br_2 was determined from the measured flow rate of known Br_2/He mixtures. The possible influence of secondary chemistry on this detection method and on the OH calibration procedure was discussed in detail in previous papers [15,16]. In the experiments conducted on the mechanistic study of reaction (1), where high concentrations of OH were used, OH radicals were directly detected at their parent peak ($m/e = 17$) with subtraction of the contribution of H_2O.

In all experiments ClO radicals were generated through the fast reaction of Cl atoms with ozone either in excess of O_3 over Cl atoms or in excess of Cl over ozone:

$$Cl + O_3 \longrightarrow ClO + O_2 \qquad (4)$$

($k_4 = 2.9 \times 10^{-11} \exp(-260/T)$ cm^3 molecule^{-1} s^{-1} [2]).

Cl atoms were formed either in a microwave discharge of Cl_2 (highly diluted in He) or by reaction of F atoms with Cl_2:

$$F + Cl_2 \longrightarrow Cl + FCl \qquad (5)$$

($k_5 = 4.8 \times 10^{-11} \exp(70/T)$ cm^3 molecule^{-1} s^{-1}).

The rate constant for reaction (5) is unpublished data from this laboratory. ClO radicals were detected at their parent peak (ClO^+, $m/e = 51$). Reaction (6), converting ClO into the NO_2 stable species, was used for the determination of the absolute concentrations of these radicals:

$$ClO + NO \longrightarrow Cl + NO_2 \qquad (6)$$

($k_6 = 6.4 \times 10^{-12} \exp(290/T)$ cm^3 molecule^{-1} s^{-1} [2]).

ClO radicals, needed for these calibration experiments, were produced through reaction (4) between ozone and excess Cl atoms. In the present study the rate constant of reaction (1) was determined from OH decay kinetics in excess of ClO radicals. Thus the accuracy of these measurements is directly related to the precision of the determination of the absolute concentrations of ClO. Another calibration method for ClO concentration was also used. Cl atoms produced in a microwave discharge of Cl_2/He mixture were converted to ClO by reaction with an excess of ozone, and the concentration of ClO radicals thus formed was derived from the dissociated fraction of Cl_2 (the net fraction of dissociated Cl_2 was around 30%): $[ClO] = [Cl]_0 = 2\Delta\,[Cl_2]$. The results obtained using the two calibration methods were in agreement within a few percent. The estimated uncertainty on the ClO-concentration measurements is $\leq$10%.

HO_2 radicals, Cl atoms, and HCl molecules were found as products of reaction (1). Cl atoms were detected at their parent peak (Cl^+, $m/e = 35$) and also as $BrCl^+$ at $m/e = 116$, after scavenging by Br_2 at the downstream end of the reactor (Br_2 was added through inlet 5) through the reaction:

$$Cl + Br_2 \longrightarrow BrCl + Br \qquad (7)$$

($k_7 = 2.3 \times 10^{-11} \exp(-135/T)$cm^3 molecule^{-1}s^{-1} [17]).

The advantage of this last procedure of Cl detection compared to direct detection of Cl (at its parent peaks, $m/e = 35/37$) was to avoid any complication arising from the contribution of Cl-containing species because of their fragmentation in the ion source of the mass spectrometer (operating at 25–30 eV). Absolute concentrations of Cl atoms could be obtained from the fraction of Cl_2 dissociated in the microwave discharge ($[Cl] = 2\Delta[Cl_2]$) and also from the fraction of Br_2 consumed in reaction (7): $[Cl] = [BrCl] = \Delta[Br_2]$. The results obtained with these methods were always consistent within a few percent.

For determining the absolute HO_2 concentrations, the fast reaction of F atoms with H_2O_2 was used as the source of HO_2 radicals, F atoms being produced in a

microwave discharge of F_2/He mixture:

$$F + H_2O_2 \longrightarrow HO_2 + HF \quad (8)$$

($k_8 = 5.0 \times 10^{-11}$ cm^3 molecule^{-1} s^{-1} ($T = 300$ K) [18]).

It was verified by mass spectrometry that more than 90% of the F_2 was dissociated in the microwave discharge. To avoid the F-atom reaction with the glass surface inside the microwave cavity, a ceramic (Al_2O_3) tube was inserted at this part of the injector. H_2O_2 was always used in excess over F atoms ([H_2O_2] $\sim 10^{13}$ molecule cm^{-3}). It should be noted that this source of HO_2 worked without constraint over the entire temperature range of the study. Absolute concentrations of HO_2 were measured using a chemical conversion of HO_2 to NO_2 through reaction (9):

$$HO_2 + NO \longrightarrow OH + NO_2 \quad (9)$$

($k_9 = 3.5 \times 10^{-12}$ exp(250/T)cm^3 molecule^{-1} s^{-1} [2]).

The concentrations used for NO ($\sim 2 \times 10^{14}$ molecule cm^{-3}) were high enough for reaction (9) to be completed before sampling into the mass spectrometer ($t \approx 5$ ms). Reaction (9) leads to simultaneous production of OH radicals. To prevent the possible HO_2 regeneration in reaction (10), calibration experiments were carried out in the presence of Br_2 in the reactor:

$$OH + H_2O_2 \longrightarrow HO_2 + H_2O \quad (10)$$

($k_{10} = 2.9 \times 10^{-12}$ exp(−160/T)cm^3 molecule^{-1} s^{-1} [2]).

Thus OH was rapidly consumed by Br_2 through reaction (3). HO_2 radicals were detected at their parent peak at $m/e = 33$ (HO_2^+). Their signals were always corrected for the contribution of H_2O_2 because of the fragmentation of H_2O_2 in the ion source. These corrections could be easily done by simultaneous detection of the signals from H_2O_2 at $m/e = 33$ and 34.

Absolute calibration of the mass-spectrometric signals of HCl (HCl^+, $m/e = 36$) was crucial in the experiments determining the branching ratio for the channel (1b). Two approaches were used to measure the absolute concentrations of HCl. The first one consisted in a calibration of the HCl signal by flowing a known HCl concentration into the reactor. In the second method, titration of H atoms by excess Cl_2 via reaction (11) was used:

$$H + Cl_2 \longrightarrow Cl + HCl \quad (11)$$

($k_{11} = 1.4 \times 10^{-10}$ exp(−590/T)cm^3 molecule^{-1}s^{-1} [19]).

Reaction (11) led to the formation of Cl atoms and HCl. Consequently, Cl atoms thus formed were titrated by excess Br_2 through reaction (7). In this case, [HCl] = $\Delta[Cl_2] = \Delta[Br_2]$, so that the concentration of HCl could be found from the consumed fraction of Cl_2 and/or Br_2. The results for HCl calibration obtained by these different methods were always consistent within 10%.

Ozone was produced by an ozonizer (Trailigaz) and was collected and stored in a trap containing silica gel at $T = 195$ K. The trap was pumped before use in order to reduce the O_2 concentration. The resulting oxygen concentration was always less than 20% of the ozone concentration introduced into the reactor. The absolute concentration of O_3 was derived using the reaction of ozone with NO, with simultaneous detection of ozone consumed and NO_2 formed ($\Delta[O_3] = \Delta[NO_2]$):

$$NO + O_3 \longrightarrow NO_2 + O_2 \quad (12)$$

($k_{12} = 2.0 \times 10^{-12}$ exp(−1400/T) cm^3 molecule^{-1} s^{-1} [2]).

O_3 could also be calibrated relative to NO_2 from the experiments on determination of ClO concentration described above. In those experiments, the initial concentration of ozone was titrated with an excess of Cl atoms, with subsequent titration of ClO formed by excess of NO leading to formation of NO_2 (reactions (4) and (6)). Assuming stoichiometric conversion of O_3 to ClO and ClO to NO_2, one has $[O_3] = [ClO] = [NO_2]$. Absolute calibrations for O_3 signals obtained from these experiments and from those based on the use of reaction (12) were consistent within a few percent.

All the relevant species (not specified above) were detected at their parent peaks: $m/e = 38$ (F_2^+), 70 (Cl_2^+), 160 (Br_2^+), 30 (NO^+), 46 (NO_2^+), 34 ($H_2O_2^+$), 18 (H_2O^+), and 48 (O_3^+). The concentrations of the stable species in the reactor were calculated from their flow rates obtained from the measurements of the pressure drop in calibrated volume flasks, with the species diluted in helium.

The purities of the gases used were as follows: He >99.9995% (Alphagaz), was passed through liquid nitrogen traps; H_2 >99.998% (Alphagaz); Cl_2 >99% (Ucar); HCl, 5% in Helium (Praxair); Br_2 >99.99% (Aldrich); F_2, 5% in Helium (Alphagaz); NO_2 >99% (Alphagaz); NO >99% (Alphagaz), purified in order to remove trace NO_2. A 70% H_2O_2 solution was purified to around 90% by continuous flowing of helium through the bubbler with H_2O_2.

RESULTS

Total Rate Constant of the OH + ClO Reaction

Two series of experiments were performed to measure the total rate constant of reaction (1), both by monitoring the OH consumption kinetics in excess of ClO radicals. ClO radicals were produced through reaction (4), which was carried out in excess of ozone over Cl atoms in the first series and in excess of Cl atoms over O_3 in the second one. Thus kinetic measurements were carried out either in the presence of excess ozone or excess Cl in the reactor. Secondary chemistry, which could not be avoided under the experimental conditions of the study and could influence the results for k_1, is different in these two cases. Therefore, the two series of experiments are presented separately below.

Measurements of k_1: Excess of Ozone in the Reactor. OH radicals were formed in reaction of H atoms (inlet 1) with NO_2 (inlet 2) and introduced into the reactor through the central tube of the sliding injector (Fig. 1). ClO radicals were produced in the reactor by reaction (4), Cl being introduced through inlet 3 and excess ozone through inlet 4. It should be noted that inlets 1, 2, and 3 were moved simultaneously, i.e. both OH and ClO sources were moved relative to the main reactor. Experiments were carried out in the temperature range 230–360 K. The ranges of the initial concentrations of the reactants, OH and ClO, are shown in Table I. The concentrations of the precursors, NO_2, O_3, and Cl_2, in the reactor were $(0.3–1.0)\times10^{13}$, $\approx2\times10^{14}$, and $(0.3–6.0)\times10^{13}$ molecule cm^{-3}, respectively. Linear flow velocities were in the range 1060–2040 cm s^{-1}. The consumption of the excess reactant, ClO radicals, was found to be negligible under the experimental conditions used. This could be expected, as (i) ClO was used in excess over OH; (ii) Cl, the main product of reaction (1), regenerated ClO in reaction with ozone; and (iii) the rate of ClO wall loss was measured to be ≤5 s^{-1}. An example of kinetic runs of the exponential decay of OH concentration measured with different excess concentrations of ClO radicals is shown in Fig. 2. Pseudo-first-order rate constants, $k_1' = -\mathrm{d}(\ln[\mathrm{OH}])/\mathrm{d}t$, obtained from such OH kinetics, should be corrected for the possible influence of the secondary and side reactions. The chemical processes occurring in the reactor under the experimental conditions used are listed in Table II. Let us note that NO ($[\mathrm{NO}] \geq [\mathrm{OH}]_0$) was formed in the source of OH radicals through reaction (2) and to a lesser extent from the sequence of reactions (13) and (14):

$$\mathrm{OH} + \mathrm{OH} \longrightarrow \mathrm{O} + \mathrm{H_2O} \qquad (13)$$

($k_{13} = 7.1 \times 10^{-13} \exp(210/T)$ cm^3 molecule^{-1} s^{-1} [16]).

$$\mathrm{O} + \mathrm{NO_2} \longrightarrow \mathrm{NO} + \mathrm{O_2} \qquad (14)$$

($k_{14} = 6.5 \times 10^{-12} \exp(120/T)$ cm^3 molecule^{-1} s^{-1} [2]).

To verify the possible influence of the processes listed in Table II on the results of the kinetic measurements, the numerical simulation of the experimental OH decays was carried out. Reaction (15) between OH

Table I Experimental Conditions and Results for the Study of the Reaction (1) in the Presence of Excess Ozone in the Reactor

Number of Decays	T(k)	[ClO]^a	[OH]^b	k_1^c
10	360	0.2–2.2	2.9–8.7	1.91 ± 0.14
8	330	0.2–2.1	2.4–5.0	1.93 ± 0.16
9	296	0.1–1.3	3.1–9.6	2.24 ± 0.10
8	255	0.1–1.2	3.1–6.5	2.57 ± 0.17
8	230	0.1–1.0	2.8–5.1	3.07 ± 0.35

[a]Units of 10^{13} molecules cm^{-3}.

[b]Units of 10^{11} molecules cm^{-3}.

[c]Units of 10^{-11} cm^3 molecules^{-1} s^{-1}; errors are twice the standard deviation and do not include systematic errors.

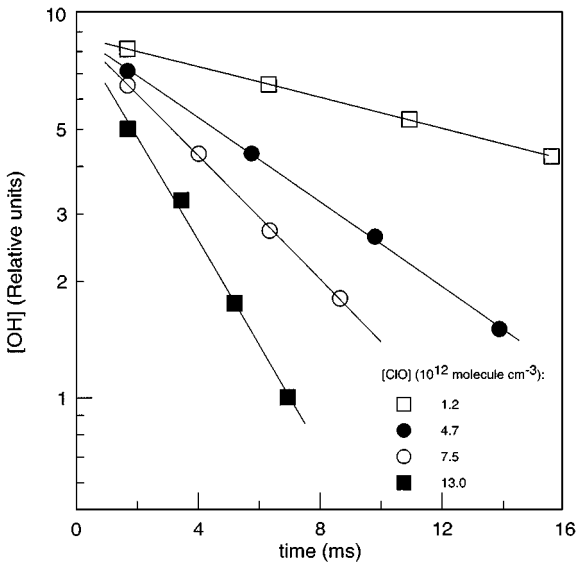

Figure 2 An example of kinetic runs of OH consumption in reaction with excess ClO ($T = 296$ K). Experiments were carried out in excess of O_3 in the reactor.

Table II Measurements of the Rate Constant of the Reaction (1): Mechanism Used in Computer Simulations

Reaction	Rate Constant[a]
$OH + ClO \rightarrow Cl + HO_2$	k_1
$OH + HO_2 \rightarrow H_2O + O_2$	4.8×10^{-11} exp(250/T)
$HO_2 + ClO \rightarrow HOCl + O_2$	4.8×10^{-13} exp(700/T)
$HO_2 + Cl \rightarrow HCl + O_2$	$4.4 \times 10^{-11} - 8.6 \times 10^{-11}$ exp(−660/T)[b]
$HO_2 + Cl \rightarrow ClO + OH$	8.6×10^{-11} exp(−660/T)
$HO_2 + NO \rightarrow OH + NO_2$	3.5×10^{-12} exp(250/T)
$ClO + NO \rightarrow Cl + NO_2$	6.4×10^{-12} exp(290/T)
$Cl + O_3 \rightarrow ClO + O_2$	2.9×10^{-11} exp(−260/T)
$OH + O_3 \rightarrow HO_2 + O_2$	1.6×10^{-12} exp(−940/T)
$OH + Cl_2 \rightarrow Cl + HOCl$	1.4×10^{-12} exp(−900/T)
$OH + wall \rightarrow loss$	(3–10) s^{-1}
$HO_2 + wall \rightarrow loss$	(4–10) s^{-1}

[a] Units are cm^3 molecule^{-1} s^{-1} for bimolecular reactions. All rate constants are from [2], except for $HO_2 + Cl$ reaction [22] and wall loss rates measured in this work.

[b] The rate constant of reaction $HO_2 + Cl \rightarrow HCl + O_2$ (18a) is presented as $k_{18a} = k_{18} - k_{18b}$.

and HO_2 (main product of reaction (1)) was found to be the most important reaction affecting the OH kinetics under the experimental conditions used:

$$OH + HO_2 \longrightarrow H_2O + O_2 \qquad (15)$$

($k_{15} = 4.8 \times 10^{-11} \exp(250/T)$ cm^3 $molecule^{-1}$ s^{-1} [2]).

The simulation procedure allowed extraction of the contribution of this reaction to the measured rates of OH decays: corrections on the originally measured values of k_1' were relatively low ($\leq$10%) at high values of k_1' and more important (up to 50%) at the lowest k_1'. This effect is mainly due to the relatively high initial concentration of OH, which makes the rate of OH consumption in reaction (15) comparable with that in reaction (1) at low concentrations of ClO radicals. However, it should be noted that the slope of the linear fit to the dependence of k_1' vs. ClO concentration (see Fig. 3), which in fact provides the value of the rate constant for reaction (1), was not significantly affected by the corrections on the individual data points for k_1'. Resulting corrections on k_1 were in the range 2–7% at the different temperatures of this study. As was noted above, the corrections on k_1' are mainly defined by the influence of reaction (15), i.e., they strongly depend on the initial concentration of OH radicals. As one can see from Fig. 3 the results obtained for k_1' at room temperature with different initial concentrations of OH are independent of $[OH]_0$, when the latter is varied by a factor of 3. This shows that the secondary reactions occurring in the reactor were

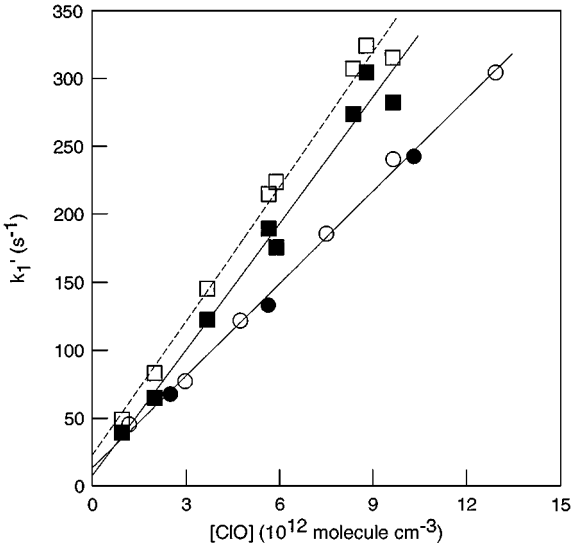

Figure 3 Example of pseudo-first-order plot of OH consumption in reaction with excess ClO radicals, and experiments were carried out in excess of ozone in the reactor. Open squares: $T = 230$ K, data obtained from the simple exponential fit to experimental kinetics; filled squares: $T = 230$ K, corrected data, from the simulation of the experimental kinetics using complete mechanism (see text); open circles: $T = 296$ K, corrected data, $[OH]_0 \approx 3.5 \times 10^{11}$ molecule cm^{-3}; filled circles: $T = 296$ K, corrected data, $[OH]_0 \approx 9.5 \times 10^{11}$ molecule cm^{-3}.

adequately taken into account. The values of k_1' were also corrected for axial and radial diffusion of OH [20]. The diffusion coefficient of OH in He was calculated from that of O in He [21]. The maximum correction on the measured values of k_1' was around 10%. The intercepts of the plots, like those presented as examples in Fig. 3, were in the range 7–20 s^{-1}, consistent with the OH decay rate measured in the absence of ClO. This OH decay rate is due to OH wall loss, OH reaction with ozone, and to a lesser extent to the slow reaction of OH with Cl_2:

$$OH + O_3 \longrightarrow HO_2 + O_2 \qquad (16)$$

($k_{16} = 1.6 \times 10^{-12} \exp(-940/T)$ cm^3 $molecule^{-1}$ s^{-1} [2])

$$OH + Cl_2 \longrightarrow Cl + HOCl \qquad (17)$$

($k_{17} = 1.4 \times 10^{-12} \exp(-900/T)$ cm^3 $molecule^{-1}$ s^{-1} [2]).

Final results for k_1 from this series of experiments are reported in Table I.

Measurements of k_1: Excess of Cl in the Reactor. In this series of experiments the configuration for the introduction of the reactants into the reactor was similar

to that described above; however, ClO radicals were produced by the reaction of O_3 with an excess of Cl atoms. The concentration of Cl atoms was (1.5–3.6) $\times 10^{13}$ molecule cm^{-3}; the ranges of the OH and ClO concentrations are presented in Table III. The flow velocity in the reactor was 1400–1850 cm s^{-1}. As in the previous case, the values of k_1' obtained from the exponential fit to the measured kinetics of OH consumption were corrected for the impact of the secondary reactions. The reaction mechanism presented in Table II was used for the numerical simulation of the OH temporal profiles. Resulting corrections on k_1 were in the range 10–28%, increasing with temperature. This could be expected as reaction (18) between HO_2 radicals and Cl atoms is the dominant process of HO_2 consumption, and the corrections on k_1 are determined, in fact, by the branching ratio for the OH + ClO forming channel (18b), which leads to OH regeneration:

$$\mathrm{Cl} + \mathrm{HO_2} \longrightarrow \mathrm{HCl} + \mathrm{O_2} \qquad (18a)$$

$$\longrightarrow \mathrm{OH} + \mathrm{ClO} \qquad (18b)$$

($k_{18} = (4.4 \pm 0.6) \times 10^{-11}$ cm^3 molecule^{-1} s^{-1}(T = 230–360 K) and $k_{18b} = 8.6 \times 10^{-11}\exp(-660/T)$cm^3 molecule^{-1} s^{-1} [22]).

The examples of the corrected pseudo-first order plots are shown in Fig. 4. As in the previous case the values of the pseudo-first order rate constants were corrected to take into account the axial and radial diffusion of OH radicals. These corrections were within 10%. Results for k_1 from this series of experiments are reported in Table III. These results are in good agreement with those obtained in the presence of excess ozone in the reactor, although the corrections applied on k_1 as a result of the secondary chemistry have opposite signs under the conditions of these two series of experiments.

All the results obtained for k_1 at different temperatures are shown in Fig. 5, together with the data

Table III Experimental Conditions and Results for the study of the Reaction (1) in the Presence of Excess Cl Atoms in the Reactor

Number of Decays	T(K)	[ClO]^a	[OH]^b	k_1^c
8	345	0.2–2.5	4.2–6.1	1.82 ± 0.23
8	300	0.2–2.1	3.3–4.7	2.18 ± 0.12
7	270	0.1–1.6	3.2–6.2	2.47 ± 0.08
8	240	0.1–0.9	2.3–5.3	3.25 ± 0.25

[a]Units of 10^{13} molecules cm^{-3}.

[b]Units of 10^{11} molecules cm^{-3}.

[c]Units of 10^{-11} cm^3 molecules^{-1} s^{-1}; errors twice the standard deviation and do not include systematic errors.

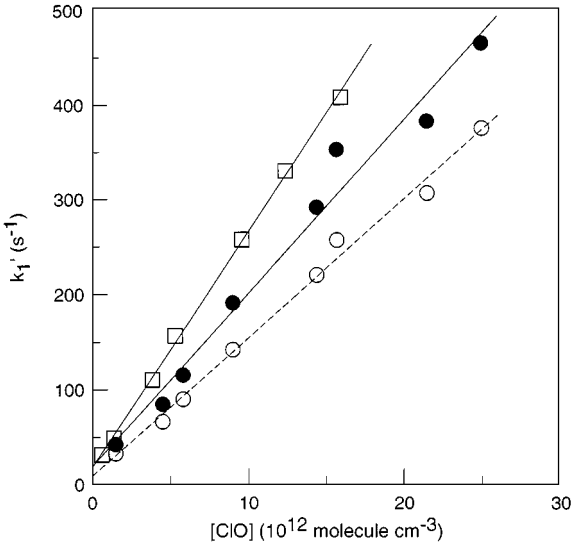

Figure 4 Example of pseudo-first-order plots of OH consumption in reaction with excess ClO radicals: experiments were carried out in excess of Cl in the reactor. Open circles: $T = 345$ K, data obtained from the simple exponential fit to experimental kinetics; filled circles: $T = 345$ K, corrected data, from the simulation of the experimental kinetics using complete mechanism (see text); open squares: $T = 270$ K, corrected data.

obtained in the most recent studies of reaction (1) [8–9,13–14]. The uncertainties on k_1 data from this study, as shown in Fig. 5, are the combination of statistical and estimated systematic errors. The estimated systematic uncertainties include ±5% for flow meter calibrations, ±1% for temperature, ±3% for pressure,

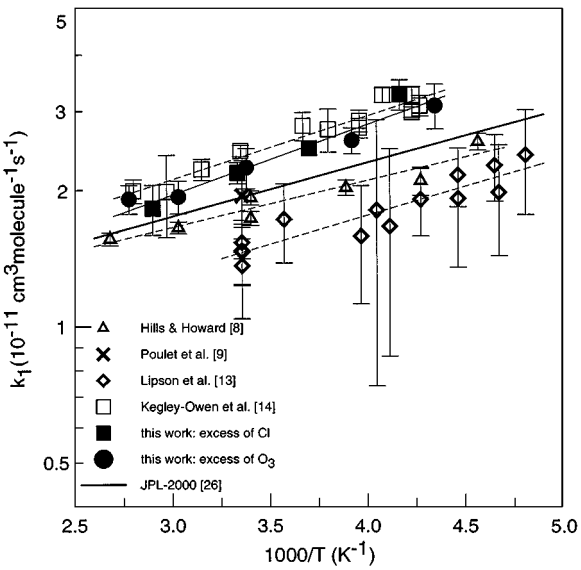

Figure 5 Temperature dependence of the total rate constant of the reaction (1).

±10% for the procedure of measuring the absolute concentrations of ClO, and ±10% for the uncertainty on k_1 as a result of the secondary chemistry. Combining these uncertainties in quadrature and adding 2σ statistical uncertainty (see Tables I and III) yields the overall uncertainty in the values of k_1 in the range 18–27%. The least-squares analysis of all the results for k_1 from the present work provides the Arrhenius expression:

$$k_1 = (6.7 \pm 1.8) \times 10^{-12} \exp\{(360 \pm 90)/T\} \text{ cm}^3 \text{ molecule}^{-1} \text{ s}^{-1}$$
$$T = 230\text{–}360 \text{ K}$$

where the quoted uncertainties represent 95% confidence limits and include estimated systematic errors.

Rate Constant of the HCl-Forming Channel (1b)

In this series of experiments, rate constant for reaction (1b) was determined from the kinetics of HCl formation. The determination of the branching ratio for the HCl-forming channel of reaction (1) represented a significant experimental challenge as (i) small amounts of the minor product HCl should be detected and quantified, and (ii) relatively high background concentrations of HCl are known to be present in the flow reactors, when working with Cl-containing species, particularly, with a microwave discharge of Cl_2. To make accurate HCl measurements, experiments were conducted by generating relatively high concentrations of HCl, i.e., by using high concentrations of the reactants OH and ClO. The disadvantage of using high initial concentrations of the reactants is that secondary reactions cannot be avoided and can significantly affect the kinetics of the minor product. To overcome this difficulty, the secondary chemistry has been quantified from the direct monitoring of the kinetics of all the species (reactants, intermediates) involved in HCl formation and consumption.

Experiments were carried out at 1-Torr total pressure and temperatures between 230 and 320 K. As in the kinetic study of reaction (1), reaction (2) in an excess of NO_2 and reaction (4) in excess ozone were used to generate OH and ClO, respectively. As noted above, relatively high initial concentrations of the reactants were used: $[OH] = (3.6\text{–}8.5) \times 10^{12}$ and $[ClO] = (0.5\text{–}2.1) \times 10^{13}$ molecule cm^{-3}. The concentrations of the precursor species were as follows: $[O_3] = (3.7\text{–}6.7) \times 10^{14}$, and $[Cl_2] = (0.3\text{–}4.4) \times 10^{13}$ molecule cm^{-3}. NO from the OH source was also present in the reactor at relatively high concentrations: $[NO]_0 = (0.9\text{–}4.4) \times 10^{13}$ molecule cm^{-3}. The kinetics of the seven species involved in this complex chemical system were observed: OH, ClO, Cl, HO_2, NO, NO_2, and HCl. An example of such experimental data observed at room temperature is presented in Figs. 6a and 6b. The reaction mechanism that was used in the simulation of the experimental curves is presented in Table IV. The good agreement (typically within a few percent) between the experimental and simulated data (for all the species except HCl) was achieved without varying any kinetic parameters. The only variable parameter, the rate constant of reaction (1b), was determined from the best fit to the kinetics

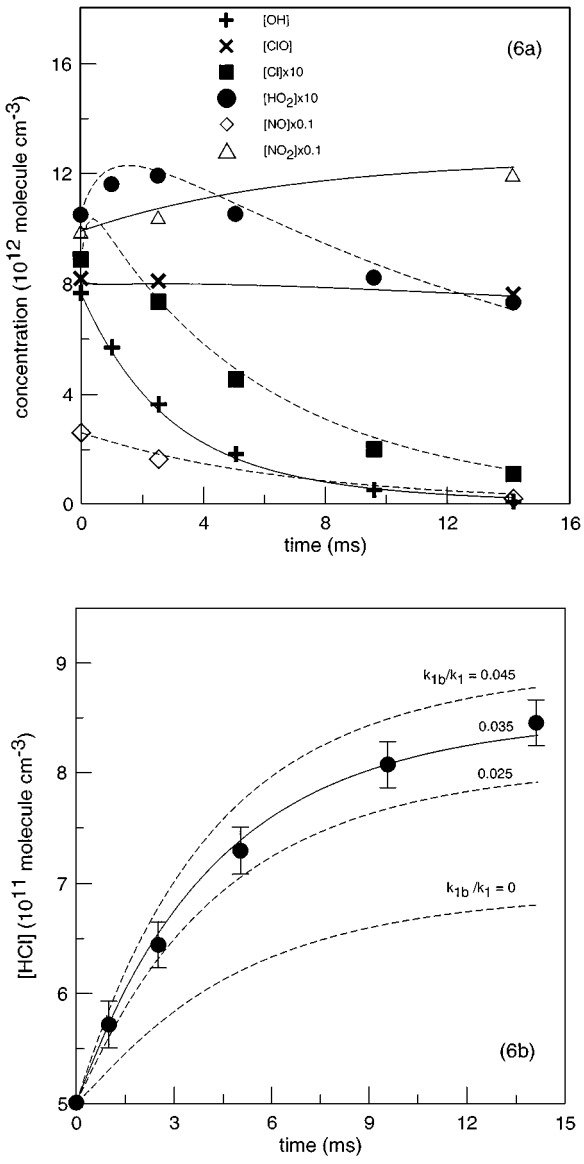

Figure 6 Example of experimental (points) and simulated (lines) kinetics for the species detected in the chemical system used for the study of the reaction (1b): $T = 298$ K, $[O_3] = 3.7 \times 10^{14}$ molecule cm^{-3}.

Table IV Measurements of the Rate Constant of the Reaction (1b)[a]

Reaction	Rate Constant[b]
$OH + ClO \rightarrow HCl + O_2$	k_{1b}, varied
$OH + ClO \rightarrow Cl + HO_2$	$k_1 - k_{1b}^c$
$OH + HO_2 \rightarrow H_2O + O_2$	4.8×10^{-11} exp(250/T)
$HO_2 + ClO \rightarrow HOCl + O_2$	4.8×10^{-13} exp(700/T)[d]
$HO_2 + Cl \rightarrow HCl + O_2$	$4.4 \times 10^{-11} - 8.6 \times 10^{-11}$ exp(−660/T)[e]
$HO_2 + Cl \rightarrow ClO + OH$	8.6×10^{-11} exp(−660/T)
$HO_2 + NO \rightarrow OH + NO_2$	3.5×10^{-12} exp(250/T)
$HO_2 + O_3 \rightarrow OH + 2O_2$	1.1×10^{-14} exp(−500/T)
$ClO + NO \rightarrow Cl + NO_2$	6.4×10^{-12} exp(290/T)
$Cl + O_3 \rightarrow ClO + O_2$	2.9×10^{-11} exp(−260/T)
$OH + O_3 \rightarrow HO_2 + O_2$	1.6×10^{-12} exp(−940/T)
$OH + Cl_2 \rightarrow Cl + HOCl$	1.4×10^{-12} exp(−900/T)
$OH + HCl \rightarrow Cl + H_2O$	2.6×10^{-12} exp(−350/T)
$OH + OH \rightarrow O + H_2O$	7.1×10^{-13} exp(210/T)
$O + OH \rightarrow H + O_2$	2.2×10^{-11} exp(120/T)
$O + HO_2 \rightarrow OH + O_2$	3.0×10^{-11} exp(200/T)
$O + ClO \rightarrow Cl + O_2$	3.0×10^{-11} exp(70/T)
$O + NO_2 \rightarrow NO + O_2$	6.5×10^{-12} exp(120/T)
$H + O_3 \rightarrow OH + O_2$	1.4×10^{-10} exp(−470/T)
$H + Cl_2 \rightarrow Cl + HCl$	1.4×10^{-10} exp(−590/T)
$H + NO_2 \rightarrow OH + NO$	4.0×10^{-10} exp(−340/T)
$OH +$ wall $\rightarrow$ loss	(3–10) s^{-1}
$HO_2 +$ wall $\rightarrow$ loss	(4–10) s^{-1}

[a] Mechanism Used in Computer Simulations.

[b] For bimolecular reactions, units are cm^3 molecule $^{-1}$ s^{-1}. All rate constants are from [2], except $HO_2 + Cl$ [22], $OH + OH$ [16], $H + Cl_2$ [19], and wall loss rates measured in this work.

[c] For k_1, the expression $k_1 = 6.7 \times 10^{-12}$ exp(360/T} cm^3 molecule $^{-1}$ s^{-1} is obtained from the present study.

[d] At temperatures $T \leq 270$ K, the HO_2 profiles were better fitted with the rate constant 7.1×10^{-12} cm^3 $molecule^{-1}$ s^{-1} (independent of temperature) as measured recently [23].

[e] The rate constant of reaction $HO_2 + Cl \rightarrow HCl + O_2$ (18a) is presented as $k_{18a} = k_{18} - k_{18b}$.

of HCl formation. Although the reaction mechanism used in the simulation of the experimental data appears to be rather complex, in fact the kinetics of HCl is defined only by two reactions: reaction (1b) and the HCl-forming channel (18a) of the secondary reaction between Cl and HO_2 (18). $H + Cl_2$ reaction can be neglected as a source of HCl since H-atom concentration is either small or scavenged by NO_2 and O_3. Reaction of HCl with OH is slow under the experimental conditions of the study and has negligible impact on the kinetics of HCl. Thus the simulated profiles of HCl are only sensitive to the rate constants of reactions (1b) and (18a) and to the concentration profiles of OH, ClO, Cl, and HO_2. All these species were directly detected and their absolute concentrations were measured. Figure 6 shows that the reaction mechanism used for the simulation gives adequate representation of the chemical processes occurring in the reactor. Similar representations were observed over the entire temperature range of the study. Figures 7a and 7b show another example of the measured and simulated kinetic data observed at the lowest temperature of the study, $T = 230$ K. Figures 6b and 7b demonstrate the sensitivity of the observed HCl profiles to the value of k_{1b} (presented as the branching ratio k_{1b}/k_1). The results of the simulation have shown that the contribution of reaction (1b) to the observed HCl-formation rate was in the range $50 \pm 10\%$ and about half of the observed HCl was due

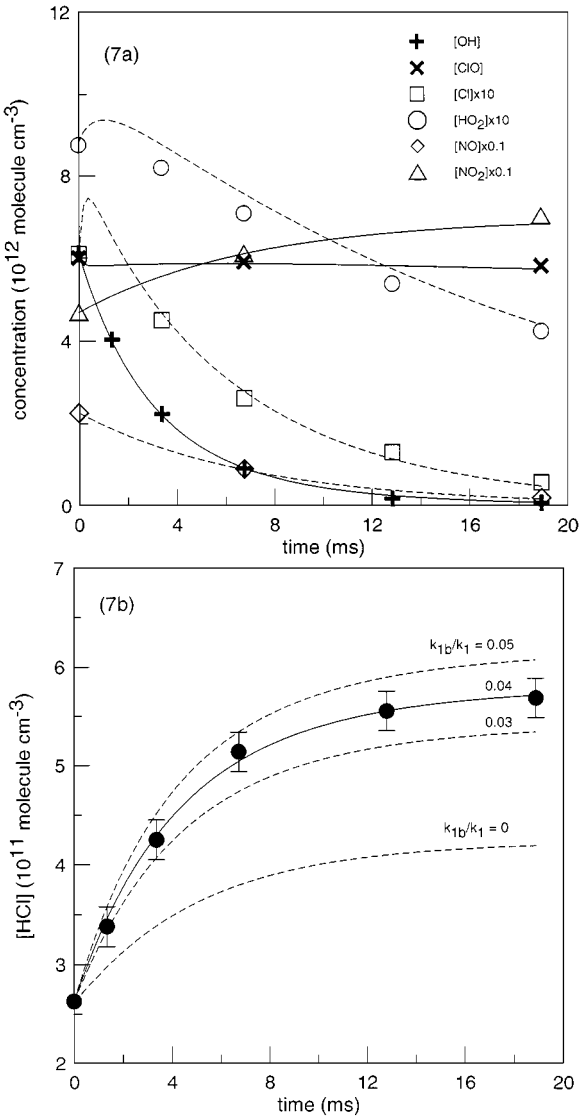

Figure 7 Example of experimental (points) and simulated (lines) kinetics for the species detected in the chemical system used for the study of the reaction (1b): $T = 230$ K, $[O_3] = 5.3 \times 10^{14}$ molecule cm^{-3}.

to reaction (18a). Thus, a precise knowledge of the rate constant for reaction (18a) is very important for an accurate determination of k_{1b}. This rate constant seems to be well established. The values of the total rate constant k_{18} determined in the three most recent studies are in excellent agreement: $k_{18} = (4.2 \pm 0.7) \times 10^{-11}$ cm^3 molecule^{-1} s^{-1}, independent of temperature in the range 250–420 K [24], $(4.45 \pm 0.06) \times 10^{-11}$ cm^3 molecule^{-1} s^{-1} for $T = 243$–368 K [25], and $(4.4 \pm 0.6) \times 10^{-11}$ cm^3 molecule^{-1} s^{-1} for $T = 230$–360 K [22]. The values of the rate constant for the minor channel (18b) of the reaction between Cl and HO_2 measured in Ref. [24] ($k_{18b} = 4.1 \times 10^{-11} \exp(-450/T)$ cm^3 molecule^{-1} s^{-1}) and in a recent study from this laboratory [22] ($k_{18b} = 8.6 \times 10^{-11} \exp(-660/T\}$ cm^3 molecule^{-1} s^{-1}) are also in good agreement (within 15% in the temperature range 230–320 K). In the simulations, the values of k_{18} and k_{18b} measured in the previous study from this laboratory were used. The relatively high contribution of reaction (18a) to HCl formation is partly due to the presence of NO in the reactor, which leads to Cl formation through reaction between ClO and NO (6) in addition to Cl formation by reaction (1a). In fact, this can be avoided if OH is formed by the reaction of F atoms with H_2O, which is NO_2- and NO-free source of the radicals. However, this method does not generate high enough concentrations of OH compared to the $H + NO_2$ reaction. Moreover, it leads to formation of O and H atoms through the sequence of reactions (13) and (19), at high OH concentrations:

$$OH + OH \longrightarrow O + H_2O \qquad (13)$$

$$O + OH \longrightarrow H + O_2 \qquad (19)$$

($k_{19} = 2.2 \times 10^{-11} \exp(120/T)$ cm^3 molecule^{-1} s^{-1} [2]).

Let us note that in the presence of NO_2, H and O atoms are scavenged in reactions (2) and (14), respectively.

Experimental conditions and results obtained for k_{1b} are reported in Table V. The initial concentrations of OH and ClO given in this table correspond to the first observation point at the top of the reaction zone. The independence of the values found for k_{1b} (see Table V, room temperature data) of the concentrations of the reactants OH and ClO, which were varied in the ranges $(3.6$–$8.2) \times 10^{12}$ and $(6.1$–$21.0) \times 10^{12}$ molecule cm^{-3} respectively, confirms that observed HCl originates from reaction (1b). Uncertainties on k_{1b} given in Table V represent 95% confidence limits of the result of the fitting procedure. Considering possible systematic errors, particularly those due to uncertainty on the rate constant of reaction (18a), the conservative 30% uncertainty can be adopted for the individual values of k_{1b} presented in the Table V. The temperature dependence of k_{1b} is shown in Fig. 8. It provides the following Arrhenius

Table V Experimental Conditions and Results for the Study of the Reaction (1b)

Expt. No.	T(K)	[ClO]^a	[OH]^a	k_{1b}^b	k_{1c}/k_1^c
1	320	6.4	8.4	5.2 ± 0.4	0.025
2	320	6.6	5.0	6.4 ± 0.3	0.031
3	298	10.8	3.6	7.9 ± 0.4	0.035
4	298	21.0	5.6	7.4 ± 1.2	0.033
5	298	10.5	5.8	7.9 ± 0.4	0.035
6	298	6.8	6.2	8.1 ± 0.6	0.036
7	298	8.2	7.7	7.9 ± 0.3	0.035
8	298	6.1	8.2	5.9 ± 0.3	0.026
9	270	8.5	4.5	9.4 ± 0.4	0.037
10	270	6.6	6.9	9.4 ± 0.4	0.037
11	250	11.0	5.0	11.2 ± 0.4	0.040
12	250	5.0	6.4	11.0 ± 0.3	0.039
13	230	13.0	4.2	14.2 ± 0.6	0.044
14	230	11.1	5.4	13.3 ± 0.5	0.041
15	230	6.0	6.1	12.6 ± 0.3	0.039
16	230	6.2	6.4	11.4 ± 0.5	0.036

[a] Concentrations are in 10^{12} molecule cm^{-3} units.

[b] Units of 10^{-13} cm^3 molecule^{-1} s^{-1}; uncertainties represent 95% confidence limits on the results of the fitting procedure and do not include possible systematic uncertainties.

[c] With $k_1 = 6.7 \times 10^{-12}$ exp (360/T} cm^3 molecule^{-1} s^{-1} from present study.

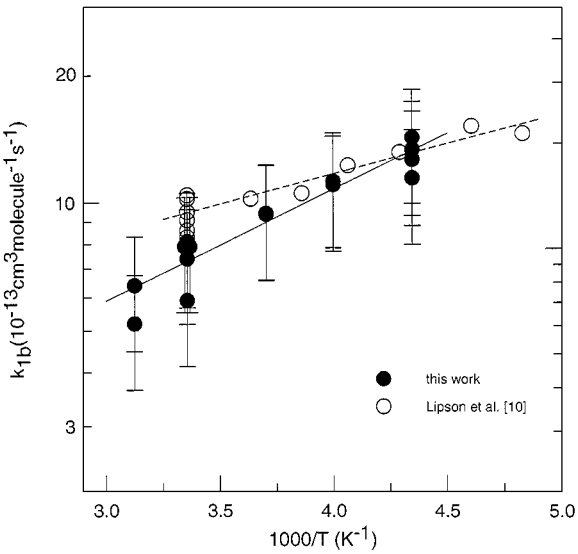

Figure 8 Temperature dependence of the rate constant for the HCl + O_2 forming channel of reaction (1). The errors shown for the data from the present study represent conservative 30% uncertainty; the uncertainties on the individual data points were not quoted in Ref. [10].

expression:

$$k_{1b} = (9.7 \pm 4.1) \times 10^{-14} \exp\{(600 \pm 120)/T\} \times \text{cm}^3\text{molecule}^{-1}\ \text{s}^{-1} \qquad T = 230\text{–}320\ \text{K}$$

where quoted uncertainties represent twice the standard deviation.

DISCUSSION

Kinetic data obtained in the present work can be compared with those from previous studies. All the data for the overall rate constant of reactions (1) are presented in Table VI and Fig. 5. As one can see, the temperature dependence of k_1 from this work is consistent within the experimental uncertainty with that measured in previous studies [8,13,14], although a somewhat higher value of $-E/R$ was observed in the present work. Our k_1 values support rather well the results of Kegley-Owen et al. [14], i.e., the highest k_1 values among those measured previously. Their $k_1(T)$ data points, shown in Fig. 5, are undistinguishable from the present results. There are two main sources for the discrepancies between the values of k_1 among different studies. These are the influence of secondary chemistry and side reactions and the measurement of the absolute concentrations of ClO radicals. These issues were discussed in detail by Kegley-Owen et al. [14] and are not considered here. A recent evaluation of the kinetic data for stratospheric modeling [26] recommends the following expressions for the specific rate constants of reactions (1): $k_{1a} = 7.4 \times 10^{-12} \exp\{(270 \pm 100)/T\}$ and $k_{1b} = 3.2 \times 10^{-13} \exp\{(320 \pm 150)/T\}$ cm^3 molecule^{-1} s^{-1}. These recommendations are based on the results of the most recent studies [8–10,13–14]. The recommended temperature dependence of $k_1 = k_{1a} + k_{1b}$ is shown in Fig. 5 for comparison.

Table VII reports all the available kinetic and mechanistic data on reactions (1a) and (1b). Although quite different Arrhenius expressions were found for k_{1b} in the present study and in Ref. [10]; the absolute values of k_{1b} determined in both studies are in good agreement (see Fig. 8), even though they were obtained under completely different experimental conditions. Experiments in Ref. [10] were carried out with very low initial concentrations of the reactants: $[\text{OH}] = (1.2\text{–}3.5) \times 10^{11}$ and $[\text{ClO}] = (4.9\text{–}8.3) \times 10^{11}$ molecule cm^{-3}. Under such experimental conditions the role of the secondary reactions is minimized and their contribution to the rate of HCl formation can be considered as negligible. Very high detection sensitivity of the mass spectrometer with chemical ionization allowed for the detection of very low concentrations of HCl formed [10]. But in the experiments of Lipson et al. [10] the signal corresponding to the concentration of HCl formed in reaction (1) was rather small compared with the background HCl signal (only 10–15% of background signal in the example of HCl kinetics presented in Ref. [10]). In the present study, much higher concentrations of the reactants were used. Under such conditions HCl formation in secondary reactions could not be avoided and should be taken into account. However, the advantage of the present experiments is that well-pronounced kinetics of HCl formation (up to twice of the background signal) could be observed under the experimental conditions used. It should be also mentioned that the procedure used in both present study and Ref. [10] led to the determination of the rate constant for channel (1b), but not of the branching ratio. In this respect, one can note that although a good agreement between values of k_{1b} of the two studies is obtained, the difference between branching ratio values k_{1b}/k_1 is significant (factor 2): $k_{1b}/k_1 = 0.035 \pm 0.010$ ($T = 230\text{–}320$ K) and 0.07 ± 0.03

Table VI Summary of the Rate Constant Data for the Reaction (1)

T (K)	P (Torr)	k_1[a] (298K)	E/R (K)	Technique[b]	Reference
298	2–3	0.91 ± 0.26		DF/RF	6
248–335	1	1.17 ± 0.33	−(66 ± 200)	DF/RF	12
243–298	1–5	1.19 ± 0.09		DF/RF	7
219–373	1	1.75 ± 0.31	−(235 ± 46)	DF/LMR	8
298	0.5–0.9	1.94 ± 0.38		DF/LIF/MS	9
205–298	100	1.46 ± 0.23	−(292 ± 72)	DF/CIMS	13
234–356	4.2–15.4	2.40 ± 0.63	−(295 ± 95)	PLP/UV/LIF	14
230–360	1	2.2 ± 0.4	−(360 ± 70)	DF/MS	This work

[a] Units of 10^{-11} cm^3 molecule^{-1} s^{-1}; uncertainties are 2σ as quoted by authors.

[b] DF = discharge flow, RF = resonance fluorescence, LMR = laser magnetic resonance, LIF = laser induced fluorescence, MS = mass spectrometry with electron impact ionization, CIMS = mass spectrometry with chemical ionization, PLP = pulsed laser photolysis, UV = UV/visible absorption.

Table VII Summary of the Kinetic and Mechanistic Data on Reactions (1a) and (1b)

T(K)	P (Torr)	Product Detected	k_{1a}/k_1	k_{1b} (cm^3 molecule^{-1} s^{-1})	Reference
298	2–3	HO_2	≥ 0.65		6
243–298	1–5	HO_2	0.85 ± 0.07		7
308	1	HO_2	0.86 ± 0.14		8
298	0.5–0.9	HCl	0.98 ± 0.12		9
207–298				3.2×10^{-13} exp (325/T)	
	100–200	HCl			10
298				$(9.5 \pm 1.6) \times 10^{-13}$	
298	20–40	HCl		$(9 \pm 3) \times 10^{-13}$	27
230–320				9.7 ± 10^{-14} exp(600/T)	
	1	HCl			This work
298				$(7.3 \pm 2.2) \times 10^{-13}$	

($T = 207$–298 K), respectively. The reason for this rather high discrepancy lies in the difference between the values of the total rate constant of reaction (1) measured in these studies. Finally, in a very recent study of Tyndall et al. [27], flash photolysis of H_2O–Cl_2–O_3 mixtures in helium with detection by tunable diode laser absorption spectroscopy has been used to study the production of HCl in reaction (1). By modeling the residual concentration of HCl, a rate coefficient $k_{1b} = (9 \pm 3) \times 10^{-13}$ cm^3 molecule^{-1} s^{-1} was obtained at room temperature. This result agrees well with the data of Lipson et al. [10] and the present determination. These results are also consistent with the current recommendation for k_{1b}, $k_{1b} = 3.2 \times 10^{-13} \exp\{(320 \pm 150)/T\}$ cm^3 molecule^{-1} s^{-1} [26], which is based on the data from Ref. [10].

In addition to kinetic parameters, thermochemical data can also be obtained from the present study since reaction (1a) is reversible:

$$OH + ClO \longleftrightarrow Cl + HO_2 \qquad (1a, 18b)$$

The forward reaction (1a) has been studied in the present work and the reverse reaction was studied recently in this laboratory [22]. First, using the activation energies for the forward and reverse reactions, one can determine the reaction enthalpy and, subsequently, the enthalpy of formation of HO_2 radicals (using known heats of formation for other species involved in the equilibrium): $\Delta H_r = E_{forward} - E_{reverse}$. Using $E_{forward} = 0.7 \pm 0.2$ kcal mol^{-1} from this work, $E_{reverse} = -(1.3 \pm 0.2)$ kcal mol^{-1} from [22], enthalpy data $\Delta H_{f,298} = 28.9$, 9.3, and 24.4 kcal mol^{-1} for Cl, OH, and ClO, respectively from Ref. [2], we obtain $\Delta H_r = -(2.0 \pm 0.4)$ kcal mol^{-1} and $\Delta H_{f,298}(HO_2) = 2.8 \pm 0.4$ kcal mol^{-1}. Another approach to the determination of the heat of formation of HO_2 radicals can be also applied. Using the expression for the equilibrium constant

$$K = k_{1a}/k_{18b} = \exp\{-(\Delta H_r - T\Delta S)/RT\}$$

with the values of k_{1a} and k_{18b} in combination with the known thermochemical data, it is possible to derive the enthalpy of reaction (1a), ΔH_r, and subsequently, $\Delta H_{f,298}(HO_2)$. Using the entropy data (in cal K^{-1} mol^{-1}) $S^\circ_{298} = 43.9$, 54.1, 39.5, and 54.4 for OH, ClO, Cl, and HO_2, respectively [2] yields $K = 2.34 \pm 0.90$, $\Delta H_r = -(1.7 \pm 0.2)$ kcal mol^{-1}, and $\Delta H_{f,298}(HO_2) = 3.1 \pm 0.2$ kcal mol^{-1}. Since we consider this method to be more precise, we recommend the value

$$\Delta H_{f,298}(HO_2) = 3.0 \pm 0.4 \text{ kcal mol}^{-1}$$

Hills and Howard [8] used the same approach to determine $\Delta H_{f,298}(HO_2)$. Using the kinetic data for k_{1a} and k_{18b} from Refs. [8,24] they obtained $\Delta H_{f,298}(HO_2) = 3.1$ and 3.0 kcal mol^{-1} from the two methods described above. Their final recommendation for the heat of formation of HO_2 radicals is identical to that from the present study, i.e., $\Delta H_{f,298}(HO_2) = 3.0 \pm 0.4$) kcal mol^{-1}. This latter value is in a good agreement with the current NASA panel recommendation, 2.8 ± 0.5 kcal mol^{-1} [2], and is somewhat lower than that recommended by IUPAC [28], 3.5 kcal mol^{-1}.

In conclusion, the kinetic information obtained in the present study leads to a more precise knowledge of the total rate constant of the OH + ClO reaction and confirms the branching ratio for HCl of a few percent under stratospheric temperatures.

BIBLIOGRAPHY

1. McElroy, J. B.; Salavitch, R. J. Science 1989, 243, 763.
2. De More, W. B.; Sander, S. P.; Golden, D. M.; Hampson, R. F.; Kurylo, M. J.; Howard, C. J.; Ravishankara, A. R.; Kolb, C. E.; Molina, M. J. Chemical Kinetics and Photochemical Data for Use in Stratospheric Modeling; NASA, JPL, California Institute of Technology: Pasadena, CA, 1997.
3. Chandra, S.; Jackman, C. H.; Douglass, A. R.; Fleming, E. L.; Considine, D. B. Geophys Res Lett 1993, 20, 351.
4. Toumi, R.; Bekki, S. Geophys Res Lett 1993, 20, 2447.
5. Dubey, M. K.; McGrath, M. P.; Smith, G. P.; Rowland, F. S. J Phys Chem A, 1998, 102, 3127.
6. Leu, M. T.; Lin, C. L. Geophys Res Lett 1979, 6, 425.
7. Burrows, J. P.; Wallington, T. J.; Wayne, R. P. J Chem Soc Faraday Trans 2: 1984, 80, 957.
8. Hills, A. J.; Howard, C. J. J Chem Phys 1984, 81, 4458.
9. Poulet, G.; Laverdet, G.; Le Bras, G. J Phys Chem 1986, 90, 159.
10. Lipson, J. B.; Beiderhase, T. W.; Molina, L. T.; Molina, M. J.; Olzmann, M. J Phys Chem A, 1999, 103, 6540.
11. Sumathi, R.; Peyerimhoff, S. D. Phys Chem Chem Phys 1999, 1, 5429.
12. Ravishankara, A. R.; Eisele, F. L.; Wine, P. H. J Chem Phys 1983, 78, 1140.
13. Lipson, J. B.; Elrod, M. J.; Beiderhase, T. W.; Molina, L. T.; Molina, M. J. J Chem Soc Faraday Trans 1997, 93, 2665.
14. Kegley-Owen, C. S.; Gilles, M. K.; Burkholder, J. B.; Ravishankara, A. R. J Phys Chem 1999, 103, 5040.
15. Bedjanian, Y.; Le Bras, G.; Poulet, G. Int J Chem Kinet 1999, 31, 698.
16. Bedjanian, Y.; Le Bras, G.; Poulet, G. J Phys Chem 1999, 103, 7017.
17. Bedjanian, Y.; Laverdet, G.; Le Bras, G. J Phys Chem A, 1998, 102, 953.
18. Walther, C. D.; Wagner, H. G. Ber Bunsen-Ges Phys Chem 1983, 87, 403.
19. Baulch, D. L.; Duxbury, J.; Grant, S. J.; Montague, D. C. J Phys Chem Ref Data 1981, 10(Suppl.), 1.
20. Kaufman, F. J Phys Chem 1984, 88, 4909.
21. Zelenov, V. V.; Kukuy, A. S.; Dodonov, A. F. Sov. J Chem Phys 1990, 5, 1109.
22. Riffault, V.; Bedjanian, Y.; Le Bras, G. Int J Chem Kinet 2001, 33, 317.
23. Knight, G. R.; Beiderhase, T.; Helleis, F.; Moortgat, G. K.; Crowley, J. N. J Phys Chem A, 2000, 104, 1674.
24. Lee, Y.-P.; Howard, C. J. J Chem Phys 1982, 77, 756.
25. Dobis, O.; Benson, S. W. J Am Chem Soc 1993, 115, 8798.
26. Sander, S. P.; Friedl, R. R.; De More, W. B.; Golden, D. M.; Kurylo, M. J.; Hampson, R. F.; Huie, R. E.; Moortgat, G. K.; Ravishankara, A. R.; Kolb, C. E.; Molina, M. J Chemical Kinetics and Photochemical Data for Stratospheric Modeling—Evaluation 13. JPL Publication No. 00-3, Pasadena, CA, 2000. (Supplement to Evaluation 12: Update of Key Reactions.)
27. Tyndal, G. S.; Kegley-Owen, C. S.; Orlando, J. J.; Fried, A. 16th International Symposium on Gas Kinetics, Cambridge, July 23–27, 2000; Book of Abstracts, PB40, University of Cambridge, 2000.
28. Atkinson, R.; Baulch, D. L.; Cox, R. A.; Hampson, R. F.; Kerr, J. A.; Rossy, M.J.; Troe, J. J Phys Chem Ref Data 1997, 26, 521.